High risk of patient self-inflicted lung injury in COVID-19 with frequently encountered spontaneous breathing patterns: a computational modelling study

Authors: Liam Weaver[1#], Anup Das[1#], Sina Saffaran[2#], Nadir Yehya[3], Timothy E. Scott[4], Marc Chikhani[8], John G. Laffey[6], Jonathan G. Hardman[5,8], Luigi Camporota[7]* and Declan G. Bates[1]*

Affiliations:

1. School of Engineering, University of Warwick, Coventry CV4 7AL, UK.
2. Faculty of Engineering Science, University College London, London, WC1E 6BT, UK.
3. Department of Anaesthesiology and Critical Care Medicine, Children's Hospital of Philadelphia, University of Pennsylvania, Philadelphia, PA, USA.
4. Academic Department of Military Anaesthesia and Critical Care, Royal Centre for Defence Medicine, ICT Centre, Birmingham B15 2SQ, UK.
5. Anaesthesia & Critical Care, Division of Clinical Neuroscience, School of Medicine, University of Nottingham, Nottingham NG7 2UH, UK.
6. Anaesthesia and Intensive Care Medicine, School of Medicine, NUI Galway, Ireland.
7. Department of Critical Care, Guy's and St Thomas' NHS Foundation Trust, London, UK.
8. Nottingham University Hospitals NHS Trust, Nottingham NG7 2UH, UK.

#Equal contributions *Co-corresponding authors: luigi.camporota@gstt.nhs.uk (+44-7876-876-952), d.bates@warwick.ac.uk (+44-2476-523-142)

Abstract

Background: There is on-going controversy regarding the potential for increased respiratory effort to generate patient self-inflicted lung injury (P-SILI) in spontaneously breathing patients with COVID-19 acute hypoxaemic respiratory failure. However, direct clinical evidence linking increased inspiratory effort to lung injury is scarce. We adapted a computational simulator of cardiopulmonary pathophysiology to quantify the mechanical forces that could lead to P-SILI at different levels of respiratory effort. In accordance with recent data, the simulator parameters were manually adjusted to generate a population of 10 patients that recapitulate clinical features exhibited by certain COVID-19 patients, i.e. severe hypoxaemia combined with relatively well-preserved lung mechanics, being treated with supplemental oxygen.

Results: Simulations were conducted at tidal volumes (VT) and respiratory rates (RR) of 7 ml/kg and 14 breaths/min (representing normal respiratory effort) and at VT/RR of 7/20, 7/30, 10/14, 10/20 and 10/30 ml/kg / breaths/min. While oxygenation improved with higher respiratory efforts, significant increases in multiple indicators of the potential for lung injury were observed at all higher VT/RR combinations tested. Pleural pressure swing increased from 12.0±0.3 cmH_2O at baseline to 33.8±0.4 cmH_2O at VT/RR of 7 ml/kg/30 breaths/min and to 46.2±0.5 cmH_2O at 10 ml/kg/30 breaths/min. Transpulmonary pressure swing increased from 4.7±0.1 cmH_2O at baseline to 17.9±0.3 cmH_2O at VT/RR of 7 ml/kg/30 breaths/min and to 24.2±0.3 cmH_2O at 10 ml/kg/30 breaths/min. Total lung strain increased from 0.29±0.006 at baseline to 0.65±0.016 at 10 ml/kg/30 breaths/min. Mechanical power increased from 1.6±0.1 J/min at baseline to 12.9±0.2 J/min at VT/RR of 7 ml/kg/30 breaths/min, and to 24.9±0.3 J/min at 10 ml/kg/30 breaths/min. Driving pressure increased from 7.7±0.2 cmH_2O at baseline to 19.6±0.2 at VT/RR of 7 ml/kg/30 breaths/min, and to 26.9±0.3 cmH_2O at 10 ml/kg/30 breaths/min.

Conclusions: Our results suggest that the forces generated by increased inspiratory effort commonly seen in COVID-19 acute hypoxaemic respiratory failure are comparable with those that have been associated with ventilator-induced lung injury during mechanical ventilation. Respiratory efforts in these patients should be carefully monitored and controlled to minimise the risk of lung injury.

Keywords: COVID-19, acute respiratory failure, hypoxaemia, patient self-inflicted lung injury, computational modelling.

Introduction

On admission, some patients with COVID-19 acute hypoxaemic respiratory failure (AHRF) exhibit profound hypoxaemia, combined with relatively preserved lung compliance and lung gas volume on CT chest imaging, and substantial increases in respiratory effort - tidal volumes (VT) of 15-20 ml/kg (1) and respiratory rates (RR) of 34 breaths/min (2) have been reported. As noted in (3), young, otherwise healthy adults can sustain tidal volumes of 20 ml/kg at a respiratory rate of 45 breaths/min almost indefinitely (4,5). There is significant debate regarding whether sustained high respiratory effort in these patients could risk causing further damage to the lungs through patient self-inflicted lung injury (P-SILI) (6-11).

Direct evidence for the existence of P-SILI in the context of purely spontaneous breathing is largely based on an animal study (12), although two studies in asthmatic children suggested that increased breathing effort could promote negative pressure pulmonary oedema (13, 14). A number of studies have also established the potential for injurious effects due to spontaneous breathing during mechanical ventilation in acute respiratory failure (15,16). In a recent study of

inspiratory effort in non-invasive ventilation, reductions in the oesophageal pressure swings (pleural pressure) of 10 cm H_2O or more after 2 hours of treatment was strongly associated with avoidance of intubation and represented the most accurate predictor of treatment success (17-19). In the context of COVID-19, a recent study has asserted an association between increased respiratory effort and worsening of respiratory function during attempts to wean patients from mechanical ventilation, although without definitively establishing a delineation between cause and effect (20,10,11). Two recent case reports also noted the existence of spontaneous pneumothorax and pneumomediastinum in COVID-19 patients, suggesting the generation of injurious transpulmonary pressures (21,22).

To obtain some additional evidence, we hypothesised that a computational model of COVID-19 pathophysiology could be used to investigate the effects of increased respiratory effort on parameters that have been associated with lung injury, namely tidal swings in pleural and transpulmonary pressure, and maximum values of mechanical power (23), driving pressure and lung strain. The aim of the study was to quantify the levels of these indicators of lung injury that are generated in our model by breathing patterns that are frequently encountered in COVID-19 patients.

Methods

Core model: The core model used in this study is a multi-compartmental computational simulator that has been previously used to simulate mechanically ventilated patients with various pulmonary disease states (24-31), including COVID-19 ARDS (32). The simulator offers several advantages, including the capability to define a large number of alveolar compartments (each with its own individual mechanical characteristics), with configurable alveolar collapse, alveolar

stiffening, disruption of alveolar gas-exchange, pulmonary vasoconstriction and vasodilation, and airway obstruction. As a result, several defining clinical features of acute lung injury can be represented in the model, including varying degrees of ventilation perfusion mismatch, physiological shunt and deadspace, alveolar gas trapping with intrinsic positive end-expiratory pressure (PEEP), collapse-reopening of alveoli etc. A detailed description of the physiological principles and mathematical equations underlying the core computational model implemented in the simulator is provided in the supplementary file. A list of key parameters in the model is given in Table S1.1 of the SM.

Adaptation to COVID-19 pathophysiology: For the current study, the model was configured to represent a patient of 70 kg ideal body weight with COVID-19 acute hypoxaemic respiratory failure, as follows.

Based on recent data [1,33-38] suggesting that some COVID-19 patients have relatively well preserved lung gas volume and compliance, the model was set to have 8% of its alveolar compartments collapsed, i.e. non-aerated. To simulate the hyperperfusion of gasless tissue reported in [1,39,40], we implemented vasodilation in the collapsed units by decreasing their vascular resistance by 80%. HPV is normally incorporated in our simulator via a mathematical function, to simulate the hypothesised disruption of HPV in COVID-19 we disabled this function in our model. We incorporated disruption of alveolar gas-exchange due to the effects of pneumonitis into the model by blocking alveolar-capillary gas equilibration in 20% of the alveolar compartments. As thrombotic complications have been reported to be a characteristic feature of COVID-19 [41,42], we also modeled the presence of microthrombi by increasing vascular resistance by a factor of 5 in 10% of the remaining compartments.

Implementing the above pathophysiological mechanisms in our model produced levels of shunt (49.5%) and deadspace (188.5 ml) leading to severe hypoxemia (SaO_2 84%, FiO_2 of 100%) consistent with recent clinical data on COVID-19 ARDS, while still maintaining relatively well preserved levels of respiratory system compliance (63 ml/cm H_2O) – see SM Table S5.1. To ensure that our results are not dependent on this particular model parameterization, we then created a "population" of 10 patients by varying the number of compartments affected by the various pathophysiological mechanisms around this nominal parameterisation, producing a range of hypoxemia/compliance levels that are still consistent with reported data; see SM, Table S5.1.

Modelling spontaneous breathing: For the current investigation, the core model was adapted to represent spontaneously breathing rather than mechanically ventilated patients. Spontaneous breathing is simulated by incorporating the variable P_{INSP}, which represents the lumped effect of chest wall, muscle and pleura on the lung. During a single respiratory cycle, P_{INSP} at time $\mathrm{t_k}$ is calculated by adapting a model developed in (43,44) based on breathing profiles of 12 patients:

$$P_{INSP}(\mathrm{t_k}) = \begin{cases} \frac{-P_{MIN}}{T_I.T_E}.\mathrm{t_k}^2 + \frac{P_{MIN}.T}{T_I.T_E}.\mathrm{t_k} & \mathrm{t_k} \in \lfloor 0, T_I \rfloor \\ \frac{P_{MIN}}{1-e^{-\frac{T_E}{\tau}}}.\left(e^{-\frac{((\mathrm{t_k}-T_I)}{\tau}} - e^{-\frac{T_E}{\tau}}\right) & \mathrm{t_k} \in \lfloor T_I, T \rfloor \end{cases}$$

The function consists of a parabolic profile during the inspiration phase of the respiratory cycle, representing the progressive increase in pressure exerted by the respiratory muscles. This is followed by an exponential profile during the expiration phase of the respiratory cycle, characterizing the passive relaxation of the muscles (a valid assumption up to a minute ventilation of 40 l/min, (45)). P_{INSP} decreases from zero to its minimum end-inspiratory value (P_{MIN}) (i.e., maximum effort) during inspiration and returns to zero at end of expiration. T is calculated from the set respiratory rate, RR, (T = 60/RR). T_I and T_E are the duration of

inspiration and expiration, such that ($T = T_I + T_E$). T_I is calculated from ($T_I = T * DC$) where DC is the duty cycle, set to 0.33. τ is the time constant of the expiratory profile and is set to T_E/RR seconds.

Calculating indices of lung injury: Pressures inside the lung are calculated in the model in an iterative fashion, as follows:

Step 1. Calculate p_i, the pressures inside each individual alveolar unit using the equation:

$$p_i(\mathrm{t_k}) = S_i(v_i(\mathrm{t_k}) - V_c)^2 + P_{ext,i} + P_{INSP} \quad \text{for } i = 1, \dots, N_A$$

The parameter S_i reflects the 'stiffness' of the compartment, $P_{ext,i}$ represents the effective net pressure acting on the alveolar compartments due to assorted localised mechanisms (e.g. oedema formation), and V_c is defined as the volume at which the alveolar compartment is considered to be 'empty', to avoid divide by 0 errors.

Step 2. Calculate P_L using the values of alveolar pressures, p_i, and airway resistances R_{Bi}, as follows: assuming zero net flow between mouth and lungs, calculate the separate alveolar flows (p_i)/ R_{Bi}, add these together to get total flow, calculate total airway resistance, and divide total flow by total airway resistance to get global lung pressure. The values of R_{Bi} are fixed and set to represent different pathophysiological mechanisms in the model.

Step 3. Calculate the respiratory system compliance C_{rs} from

$$C_{rs} = \frac{VT}{\Delta P_L} \qquad [1]$$

where VT is the tidal volume, and ΔP_L is the difference between the minimum lung pressure and end expiratory lung pressure. Note that Equation 1 gives us C_{rs}, rather than C_L, because we are

applying P_{ext} and P_{INSP} to the alveoli directly (an anatomical modeling simplification but of no consequence mathematically).

Step 4. Calculate the dynamic lung compliance C_L

Since $EL_{rs} = EL_L + EL_{cw}$, we have that $\frac{1}{C_L} = \frac{1}{C_{rs}} - \frac{1}{C_{cw}}$

where C_{cw} is the chest wall compliance (set to 144 mL/cmH_2O based on data from COVID-19 patients in (46)) and C_{rs} has been found from Eq. 1.

Step 5. Calculate transpulmonary pressure P_{tp} (equivalent to lung stress (47))

Since $C_L = \frac{\Delta V}{\Delta P_{tp}}$, then

$$P_{tp} = \frac{\Delta V}{C_L} \qquad [2]$$

if $\Delta P_{tp} = P_{tp} - 0$, and ΔV is the difference between the current lung volume and the unstressed volume of the lung (the residual volume, set to 1.2L).

Step 6. Calculate pleural pressure P_{pl} from: $P_{pl} = P_L - P_{tp}$

Step 7. Calculate the mechanical power applied to the lungs as the energy per breath (defined as the area of the triangle enclosed by the inspiratory limb of the ΔP_{tp} pressure-volume curve and the change in volume, i.e. $0.5 \times VT \times \Delta P_{tp}$, in Joules) multiplied by RR, as described in (48).

Step 8. Calculate driving pressure ΔP as $\Delta P = VT \times EL_{RS} = \Delta P_L$ (from Equation 1).

Step 9. Calculate the total lung strain as the sum of dynamic and static strain (49), where

dynamic strain $= \frac{VT}{EELV\ at\ \text{VT / RR of 7ml/kg / 14 breaths/min}}$

static strain $= \frac{EELV - EELV\ at\ \text{VT / RR of 7ml/kg / 14 breaths/min}}{EELV\ at\ \text{VT / RR of 7ml/kg / 14 breaths/min}}$.

To observe the various pulmonary effects of interest, the following values were also computed and recorded: arterial oxygen partial pressure (PaO_2), arterial carbon dioxide partial pressure ($PaCO_2$), physiological shunt, calculated using the classical shunt equation, based on the calculated values of arterial, pulmonary end-capillary and mixed venous O_2 content. Physiological deadspace (and deadspace fraction; VD/VT) were calculated from $PaCO_2$, mixed expired CO_2 pressure ($P\bar{E}CO_2$) and the exhaled tidal volume.

All model simulations were run for 30 minutes, with the reported data averaged over the final 1 minute, and conducted using Matlab version R2019b.v9 (MathWorks Inc., Natick, MA, USA).

Results

The simulated patient population replicates levels of hypoxaemia that have frequently been reported in spontaneously breathing COVID-19 patients. SaO_2, PaO_2 and $PaCO_2$ on 100% oxygen at baseline were 83.8±5.1%, 52.6±7.1 mmHg, and 51.8±1.5 mmHg, respectively (Table 1). Oxygenation improved at higher respiratory efforts (SaO_2 of 97.6±0.8 at VT / RR of 10 ml/kg / 30 breath/min) and $PaCO_2$ decreased. Values of respiratory system compliance and end-expiratory lung volume (EELV) at baseline were 63±1.4 ml/cmH_2O and 1678.9±35.3 ml, showing good agreement with the data for a cohort of COVID-19 patients reported in a recent study (38). Compliance reduced significantly at higher respiratory rates (to 25±0.3 ml/cmH_2O at VT / RR of 7 ml/kg / 30 breath/min). Physiological shunt and deadspace were decreased and increased, respectively, at higher respiratory effort.

Inspiratory pressures required to generate the different increased breathing patterns (maximum P_{MIN} of 35.4±0.2 cmH_2O at VT / RR of 10 ml/kg / 30 breath/min) were well within the limits

specified for a 70kg adult male (P_{MIN} of 78.5 cmH_2O at age 60, and 108.9 cmH_2O at age 40, (50)).

As shown in Table 1 and Figure 1, significant increases in multiple indicators of the potential for lung injury were observed at all higher VT / RR combinations tested. Pleural pressure swing increased from 12.0±0.3 cmH_2O at baseline to 33.8±0.4 cmH_2O at VT/RR of 7 ml/kg / 30 breaths/min and to 46.2±0.5 cmH_2O at 10 ml/kg / 30 breaths/min. Transpulmonary pressure swing increased from 4.7±0.1 cmH_2O at baseline to 17.9±0.3 cmH_2O at VT/RR of 7 ml/kg / 30 breaths/min and to 24.2±0.3 cmH_2O at 10 ml/kg / 30 breaths/min. Total lung strain increased from 0.29±0.006 at baseline to 0.65±0.016 at 10 ml/kg / 30 breaths/min. Mechanical power increased from 1.6±0.1 J/min at baseline to 12.9±0.2 J/min at VT/RR of 7 ml/kg / 30 breaths/min, and to 24.9±0.3 J/min at 10 ml/kg / 30 breaths/min. Driving pressure increased from 7.7±0.2 cmH_2O at baseline to 19.6±0.2 at VT/RR of 7 ml/kg / 30 breaths/min, and 26.9±0.3 cmH_2O at 10 ml/kg / 30 breaths/min.

The effect of increased respiratory effort on the distribution of maximum compartmental volumes in the model is shown in Fig. S4.1 and Fig. S4.2 in the supplementary file. As shown, at the higher values of tidal volume and respiratory rate, the proportion of model compartments experiencing larger maximum volumes is significantly increased.

Discussion

During mechanical ventilation, the power required to inflate the lungs is provided by an external source of energy, whereas during spontaneous unassisted breathing it is provided by the respiratory muscles. However, as pointed out in (51), lung injury (in the sense of mechanical

lesions in the interstitial space due to microfractures of the extracellular matrix or the capillary walls) arises from the mechanical energy applied to the lungs, which generates the relevant pressures. There is therefore no reason to believe that the extent of injury will be significantly different whether excessive pressures are generated by respiratory muscles in spontaneous breathing or by a mechanical ventilator. Similarly to the case of VILI, there is also no reason to expect that, in the case of injured lungs, forces generated by respiratory muscles could not lead to injurious effects on a regional level due to lung heterogeneity. This may be a particular concern in the case of COVID-19 AHRF, since current understanding of the underlying pathophysiology points to a strongly heterogeneous lung profile incorporating alveolar collapse, oedema, and significant vascular derangement.

As well as increases in transpulmonary pressure swings, we also observed large increases in pleural pressure swings at higher respiratory effort, up to a maximum of 46.2±0.5 cmH_2O. As discussed in (16), negative alveolar pressures created by large changes in pleural pressure, and therefore positive changes in transvascular pressure, favour lung oedema, a mechanism that is amplified with increased vascular permeability, (52, 53). Given that negative pressures from diaphragm contraction are not distributed uniformly, there is also the potential to cause pendelluft gas movement due to localised changes in pleural pressures in dependent regions, (54). Finally, it is important to recognise that when dynamic systems (from aircraft engines to human lungs) are subjected to repeated cycles of excessive stresses and strains, their deterioration over time is often not linear; rather, damage can accumulate “silently” before eventually manifesting and spreading rapidly (55).

In light of the above considerations, it is difficult to see how, for a respiratory effort that a patient (and their treating clinician) might consider tolerable, the levels of transpulmonary/pleural

pressure swings, driving pressure and mechanical power produced in our model (Table 1) could be regarded as safe. Certainly, it is unlikely that any mechanical ventilation strategy that produced similar values would be considered "protective" according to current standard guidelines. Our results also highlight that improvements in PaO_2/FiO_2 ratio associated with larger tidal volumes and respiratory rates should be interpreted in the context of the associated increased respiratory effort, and are not necessarily expressions of improved lung condition. Indeed, the improvement in PaO_2/FiO_2 ratio we observed at higher respiratory effort was coupled with reduced lung compliance and the development of levels of mechanical power associated with worse short (56, 57) and long term (58) survival.

Our study has a number of limitations. The results are based on computational modelling of mechanisms that have been proposed to underlie COVID-19 pathophysiology, rather than on models matched to individual data from patients with COVID-19. Accordingly, many model parameters were manually adjusted to give overall outputs that are similar to reported data on COVID-19 patients, rather than being fit to data that explicitly defines the parameters. The model also neglects some physiological realities (namely interdependence of alveoli, non-uniformity of diaphragm contraction, and gravitational effects), however, it seems reasonable to expect that inclusion of these effects would act to produce even higher localised values of the reported lung injury indices in certain lung regions. Due to a lack of data we have also not modelled the potential effects of variations in the ratio of inspiratory/expiratory time at higher respiratory rates.

Our results are limited to the case of purely spontaneous breathing with oxygen support – consideration of the effects of high respiratory effort during positive pressure non-invasive

ventilation (CPAP, BIPAP, etc) is an important open question, but requires further development of the model and will be the subject of future studies.

Investigating the issues raised here in clinical trials is likely to prove challenging both from an ethical and practical point of view, and suitable animal models of COVID-19 pathophysiology with which to study these questions are yet to emerge (59). In these circumstances, we hope that insights from detailed computational models that recapitulate patient breathing patterns and lung mechanics can provide useful evidence with which to inform current and future debates (60).

Conclusions

Our results indicate that transpulmonary and pleural pressure swings, and levels of driving pressure, lung strain and mechanical power that have been associated with VILI during mechanical ventilation can develop in spontaneously breathing patients with COVID-19 acute respiratory failure, at levels of respiratory effort that are being frequently encountered by clinicians. Respiratory efforts in these patients should be carefully monitored and controlled to minimise the risk of lung injury.

Supplementary Materials

AIC_Supplementary.pdf – Full description of computational simulator, additional results and figures.

Funding

UK Engineering and Physical Sciences Research Council (grants EP/P023444/1 and EP/V014455/1).

Competing interests

The authors declare that they have no competing interests.

Availability of data and materials

All data for the study is contained in the paper and the SM. Requests to be forwarded to Prof. Declan G Bates.

Ethics approval and consent to participate

Not applicable

Consent for publication

Not applicable

Authors' contributions

DGB designed the study. AD, LW and SS performed the modelling and carried out simulations. All authors contributed to the modelling, analysed the data, and contributed to writing the paper.

Acknowledgements

Not applicable.

Authors' information (optional)

Not applicable.

References

1. Gattinoni L, Chiumello D, Caironi P, Busana M, Romitti F, Brazzi L, et al. COVID-19 pneumonia: different respiratory treatments for different phenotypes? Intensive Care Med. 2020;46(6):1099-102.

2. Fazzini B, Fowler AJ, Zolfaghari P. Effectiveness of prone position in spontaneously breathing patients with COVID-19: A prospective cohort study. *Journal of the Intensive Care Society*. 2021; doi:10.1177/1751143721996542.

3. Komorowski M, Aberegg SK, Using applied lung physiology to understand COVID-19 patterns. British Journal of Anaesthesia, 2020; 125 (3):250e253.

4. Kapitan KS. Ventilatory failure. Can you sustain what you need? Ann Am Thorac Soc. 2013;10:396e914.

5. Freedman S. Sustained maximum voluntary ventilation. Respir Physiol. 1970;8:230e44.

6. Gattinoni L, Marini JJ, Busana M, Chiumello D, Camporota L. Spontaneous breathing, transpulmonary pressure and mathematical trickery. Ann Intensive Care. 2020;10(1):88.

7. Tobin MJ, Laghi F, Jubran A. P-SILI is not justification for intubation of COVID-19 patients. Ann Intensive Care. 2020;10(1):105.

8. Tobin MJ, Jubran A, Laghi F. P-SILI as justification for intubation in COVID-19: readers as arbiters. Ann Intensive Care. 2020;10(1):156.

9. Cruces P, Retamal J, Hurtado DE, Erranz B, Iturrieta P, Gonzalez C, et al. A physiological approach to understand the role of respiratory effort in the progression of lung injury in SARS-CoV-2 infection. Crit Care. 2020;24(1):494.

10. Gattinoni L, Marini JJ, Camporota L. The Respiratory Drive: An Overlooked Tile of COVID-19 Pathophysiology. Am J Respir Crit Care Med. 2020;202(8):1079-80.

11. Tobin MJ, Jubran A, Laghi F. Respiratory Drive Measurements Do Not Signify Conjectural Patient Self-inflicted Lung Injury. Am J Respir Crit Care Med. 2021;203(1):142-3.

12. Mascheroni D, Kolobow T, Fumagalli R, Moretti MP, Chen V, Buckhold D. Acute respiratory failure following pharmacologically induced hyperventilation: an experimental animal study. Intensive Care Med. 1988;15(1):8-14.

13. Dunnill MS. The pathology of asthma, with special reference to changes in the bronchial mucosa. J Clin Pathol. 1960;13:27-33.

14. Stalcup SA, Mellins RB. Mechanical forces producing pulmonary edema in acute asthma. N Engl J Med. 1977;297(11):592-6.

15. Yoshida T, Uchiyama A, Matsuura N, Mashimo T, Fujino Y. The comparison of spontaneous breathing and muscle paralysis in two different severities of experimental lung injury. Crit Care Med 2013;41:536–545.

16. Brochard L, Slutsky A, Pesenti A, Mechanical Ventilation to Minimize Progression of Lung Injury in Acute Respiratory Failure. Am J Respir Crit Care Med. 2017;195(4):438-442.

17. Tonelli R, Fantini R, Tabbi L, Castaniere I, Pisani L, Pellegrino MR, et al. Early Inspiratory Effort Assessment by Esophageal Manometry Predicts Noninvasive Ventilation Outcome in De Novo Respiratory Failure. A Pilot Study. Am J Respir Crit Care Med. 2020;202(4):558-67.

18. Yoshida T. The Dark Side of Spontaneous Breathing during Noninvasive Ventilation. From Hypothesis to Theory. Am J Respir Crit Care Med. 2020;202:4,482-484.

19. Kumar Jha A. Continued Vigorous Inspiratory Effort as a Predictor of Noninvasive Ventilation Failure. Am J Respir Crit Care Med. 2020;202:12, 1738-1739.

20. Esnault P, Cardinale M, Hraiech S, Goutorbe P, Baumstrack K, Prud'homme E, et al. High Respiratory Drive and Excessive Respiratory Efforts Predict Relapse of Respiratory Failure in Critically Ill Patients with COVID-19. Am J Respir Crit Care Med. 2020;202(8):1173-8.

21. Alharthy A, Bakirova GH, Bakheet H, Balhamar A, Brindley PG, Alqahtani SA, et al. COVID-19 with spontaneous pneumothorax, pneumomediastinum, and subcutaneous emphysema in the intensive care unit:Two case reports. J Infect Public Health. 2020;14(3):290-2.

22. Rafiee MJ, Babaki Fard F, Samimi K, Rasti H, Pressacco J. Spontaneous pneumothorax and pneumomediastinum as a rare complication of COVID-19 pneumonia: Report of 6 cases. Radiol Case Rep. 2021;16(3):687-92.

23. Cressoni M et al. Mechanical Power and Development of Ventilator-induced Lung Injury. Anesthesiology. 2016;124(5):1100-8.

24. McCahon R, Columb M, Mahajan R, Hardman J. Validation and application of a high-fidelity, computational model of acute respiratory distress syndrome to the examination of the indices of oxygenation at constant lung-state. Br J Anaesth. 2008;101(3):358-65.

25. Das A, Cole O, Chikhani M, Wang W, et al. Evaluation of lung recruitment maneuvers in acute respiratory distress syndrome using computer simulation. Critical Care. 2015;19(1):8.

26. Chikhani M, Das A, Haque M, Wang W, Bates DG, Hardman JG. High PEEP in acute respiratory distress syndrome: quantitative evaluation between improved arterial oxygenation and decreased oxygen delivery. Br J Anaesth. 2016;117(5):650-8.

27. Das A, Haque M, Chikhani M, Cole O, Wang W, Hardman JG, et al. Hemodynamic effects of lung recruitment maneuvers in acute respiratory distress syndrome. BMC Pulm Med. 2017;17(1):34.

28. Das A, Camporota L, Hardman JG, Bates DG. What links ventilator driving pressure with survival in the acute respiratory distress syndrome? A computational study. Respir Res. 2019;20(1):29.

29. Saffaran S, Das A, Hardman JG, Yehya N, Bates DG. High-fidelity computational simulation to refine strategies for lung-protective ventilation in paediatric acute respiratory distress syndrome. Intensive Care Med. 2019;45(7):1055-7.

30. Saffaran S, Das A, Laffey JG, Hardman JG, Yehya N, Bates DG. Utility of Driving Pressure and Mechanical Power to Guide Protective Ventilator Settings in Two Cohorts of Adult and Pediatric Patients With Acute Respiratory Distress Syndrome: A Computational Investigation. Crit Care Med. 2020;48(7):1001-8.

31. Scott TE, Haque M, Das A, Cliff I, Bates DG, Hardman JG. Efficacy of continuous positive airway pressure in casualties suffering from primary blast lung injury: A modeling study. Annu Int Conf IEEE Eng Med Biol Soc. 2019;2019:4965-8.

32. Das A, Saffaran S, Chikhani M, Scott TE, Laviola M, Yehya N, et al. In Silico Modeling of Coronavirus Disease 2019 Acute Respiratory Distress Syndrome: Pathophysiologic Insights and Potential Management Implications. Crit Care Explor. 2020;2(9):e0202.

33. Gattinoni L, Coppola S, Cressoni M, Busana M, Rossi S, Chiumello D. COVID-19 Does Not Lead to a "Typical" Acute Respiratory Distress Syndrome. Am J Respir Crit Care Med. 2020;201(10):1299-300.

34. Marini JJ, Gattinoni L. Management of COVID-19 Respiratory Distress. JAMA. 2020;323(22):2329-30.

35. Roesthuis L, van den Berg M, van der Hoeven H. Advanced respiratory monitoring in COVID-19 patients: use less PEEP! Crit Care. 2020;24(1):230.

36. Tsolaki V, Siempos I, Magira E, Kokkoris S, Zakynthinos GE, Zakynthinos S. PEEP levels in COVID-19 pneumonia. Crit Care. 2020;24(1):303.

37. Bonny V, Janiak V, Spadaro S, Pinna A, Demoule A, Dres M. Effect of PEEP decremental on respiratory mechanics, gasses exchanges, pulmonary regional ventilation, and hemodynamics in patients with SARS-Cov-2-associated acute respiratory distress syndrome. Crit Care. 2020;24(1):596.

38. Chiumello D, Busana M, Coppola S, Romitti F, Formenti P, Bonifazi M, et al. Physiological and quantitative CT-scan characterization of COVID-19 and typical ARDS: a matched cohort study. Intensive Care Med. 2020;46(12):2187-96.

39. Lang M, Som A, Mendoza DP, Flores EJ, Reid N, Carey D, et al. Hypoxaemia related to COVID-19: vascular and perfusion abnormalities on dual-energy CT. Lancet Infect Dis. 2020;20(12):1365-6.

40. Albarello F, Pianura E, Di Stefano F, Cristofaro M, Petrone A, Marchioni L, et al. 2019-novel Coronavirus severe adult respiratory distress syndrome in two cases in Italy: An uncommon radiological presentation. Int J Infect Dis. 2020;93:192-7.

41. Helms J, Tacquard C, Severac F, Leonard-Lorant I, Ohana M, Delabranche X, et al. High risk of thrombosis in patients with severe SARS-CoV-2 infection: a multicenter prospective cohort study. Intensive Care Med. 2020;46(6):1089-98.

42. Menter T, Haslbauer JD, Nienhold R, Savic S, Hopfer H, Deigendesch N, et al. Postmortem examination of COVID-19 patients reveals diffuse alveolar damage with severe capillary congestion and variegated findings in lungs and other organs suggesting vascular dysfunction. Histopathology. 2020;77(2):198-209.

43. Mecklenburgh JS, Mapleson WW. Ventilatory assistance and respiratory muscle activity. 2: Simulation with an adaptive active (“aa” or “a-squared”) model lung. Br J Anaesth. 1998;80(4):434-9.

44. Albanese A, Cheng L, Ursino M, Chbat NW. An integrated mathematical model of the human cardiopulmonary system. Am J Physiol Heart Circ Physiol, 2016; 310(7):H899-921.

45. Comroe JH. Mechanical factors in breathing. In:Physiology of Respiration. Chicago: Year Book Medical Publishers, 1977, chapt. 10, p. 91–141.

46. Haudebourg A-F, Perier F, Tuffet S, de Prost N, Razazi K, Mekontso Dessap A, Carteaux G, Respiratory Mechanics of COVID-19- versus Non-COVID-19-associated Acute Respiratory Distress Syndrome. Am J Respir Crit Care Med, 2020;202(2):287-290.

47. Eikermann M, Vidal Melo M, Therapeutic Range of Spontaneous Breathing during Mechanical Ventilation. Anesthesiology, 2014;(120):536–539.

48. Cressoni M et al. Mechanical Power and Development of Ventilator-induced Lung Injury. Anesthesiology. 2016;124(5):1100-8.

49. Protti A, Votta E, Gattinoni L. Which is the most important strain in the pathogenesis of ventilator-induced lung injury. Curr Opin Crit Care. 2014;20:33–8.

50. Harik-Khan RI, Wise RA, Fozard JL. Determinants of maximal inspiratory pressure. The Baltimore Longitudinal Study of Aging. Am J Respir Crit Care Med. 1998;158(5 Pt 1):1459-64.

51. Gattinoni L. Ventilation-induced lung injury exists in spontaneously breathing patients with acute respiratory failure: We are not sure. Intensive Care Med. 2017;43(2):256-8.

52. Grieco DL, Menga LS, Eleuteri D, Antonelli M. Patient self-inflicted lung injury: implications for acute hypoxemic respiratory failure and ARDS patients on non-invasive support. Minerva Anestesiol. 2019;85(9):1014-23.

53. Arnal JM, Chatburn R. Paying attention to patient self-inflicted lung injury. Minerva Anestesiol. 2019;85(9):940-2.

54. Yoshida T, Roldan R, Beraldo MA, Torsani V, Gomes S, De Santis RR, et al. Spontaneous Effort During Mechanical Ventilation: Maximal Injury With Less Positive End-Expiratory Pressure. Crit Care Med. 2016;44(8):e678-88.

55. Bhat S, Patibandla R. Metal fatigue and basic theoretical models: a review. Alloy Steel-Properties and Use. 2011;22.

56. Neto AS, Deliberato RO, Johnson AE, Bos LD, Amorim P, Pereira SM, et al. Mechanical power of ventilation is associated with mortality in critically ill patients: an analysis of patients in two observational cohorts. Intensive care medicine. 2018;44(11):1914-22.

57. Zhang Z, Zheng B, Liu N, Ge H, Hong Y. Mechanical power normalized to predicted body weight as a predictor of mortality in patients with acute respiratory distress syndrome. Intensive Care Med. 2019;45(6):856-64.

58. Parhar KKS, Zjadewicz K, Soo A, Sutton A, Zjadewicz M, Doig L, et al. Epidemiology, Mechanical Power, and 3-Year Outcomes in Acute Respiratory Distress Syndrome Patients Using Standardized Screening. Ann Am Thorac Soc. 2019;16(10):1263-72.

59. Ehaideb SN, Abdullah ML, Abuyassin B, Bouchama A. Evidence of a wide gap between COVID-19 in humans and animal models: a systematic review. Critical Care. 2020;24(1):1-23.

60. Tonelli R, Marchioni A, Tabbì L, Fantini R, Busani S, Castaniere I, Andrisani D, Gozzi F, Bruzzi G, Manicardi L, et al. Spontaneous Breathing and Evolving Phenotypes of Lung Damage in Patients with COVID-19: Review of Current Evidence and Forecast of a New Scenario. J. Clin. Med. 2021;10,975.

Figure Legends

Figure 1: Inspiratory, pleural, transpulmonary and alveolar pressure swings generated by normal and increased respiratory effort in our COVID-19 model (patient 1 – see SM Table S5.1), (A) VT = 7 ml/kg, RR = 14 b/min, (B) VT = 10 ml/kg, RR = 14 b/min, (C) VT = 7 ml/kg, RR = 20 b/min, (D) VT = 10 ml/kg, RR = 20 b/min, (E) VT = 7 ml/kg, RR = 30 b/min, (F) VT = 10 ml/kg, RR = 30 b/min.

	VT = 7 (ml/kg) RR = 14 (bpm)	VT = 7 (ml/kg) RR = 20 (bpm)	VT = 7 (ml/kg) RR = 30 (bpm)	VT = 10 (ml/kg) RR = 14 (bpm)	VT = 10 (ml/kg) RR = 20 (bpm)	VT = 10 (ml/kg) RR = 30 (bpm)
P_{MIN} (cmH$_2$O)	-12.4±0.3	-17.4±0.3	-25.3±0.2	-17.8±0.4	-24.5±0.4	-35.4±0.2
SaO$_2$ (%)	83.8±5.1	84.1±5	93.5±1.4	84.1±5	89.7±2.3	97.6±0.8
PaO$_2$ (mmHg)	52.6±7.1	49.2±6.2	66.7±4.7	48.9±6.3	55.8±4.4	98.4±13.2
PF ratio (mmHg)	52.6±7.1	49.2±6.2	66.7±4.7	48.9±6.3	55.8±4.4	98.4±13.2
Phys. Shunt (%)	48.9±4.7	48.8±4.7	38.5±1.7	48.8±4.7	43.5±2.6	31.7±1.7
Phys. VD (ml)	187.4±5.6	185.6±6.6	187±4.5	258.5±10.5	255±8.6	255.1±6.6
VD/VT	0.38±0.01	0.38±0.01	0.38±0.01	0.37±0.02	0.37±0.01	0.37±0.01
PaCO$_2$ (mmHg)	51.8±1.5	37.3±1.6	25±0.6	36.4±1.5	25.9±0.8	17.2±0.4
EELV (ml)	1678.9±35.3	1773.5±36.3	1933.6±37.3	1718.8±35.7	1844.9±34.5	2064.6±31
VT (ml)	487.7±2.1	487.9±2.2	489.6±0.7	695.9±1.9	695±2.8	697.5±1.3
Compliance (ml/cmH$_2$O)	63±1.4	39.6±0.9	25±0.3	64.7±1.4	41.3±0.7	26±0.3
DP (cmH$_2$O)	7.7±0.2	12.3±0.2	19.6±0.2	10.8±0.2	16.8±0.3	26.9±0.3
Power (J/min)	1.6±0.1	4.7±0.1	12.9±0.2	3.0±0.1	8.9±0.2	24.9±0.3
Total Strain	0.29±0.006	0.35±0.005	0.44±0.008	0.44±0.008	0.51±0.011	0.65±0.016
ΔP_{PL} (cmH$_2$O)	12.0±0.3	21.6±0.5	33.8±0.4	16.8±0.4	29.2±0.5	46.2±0.5
ΔP_{TP} (cmH$_2$O)	4.7±0.1	9.8±0.2	17.9±0.3	6.3±0.2	13.1±0.3	24.2±0.3

Table 1: Oxygenation, lung mechanics, maximum pressure swings, and other injury indicators generated in our COVID-19 model for different levels of respiratory effort on 100% oxygen, data presents mean ± sd across the population of 10 patients.

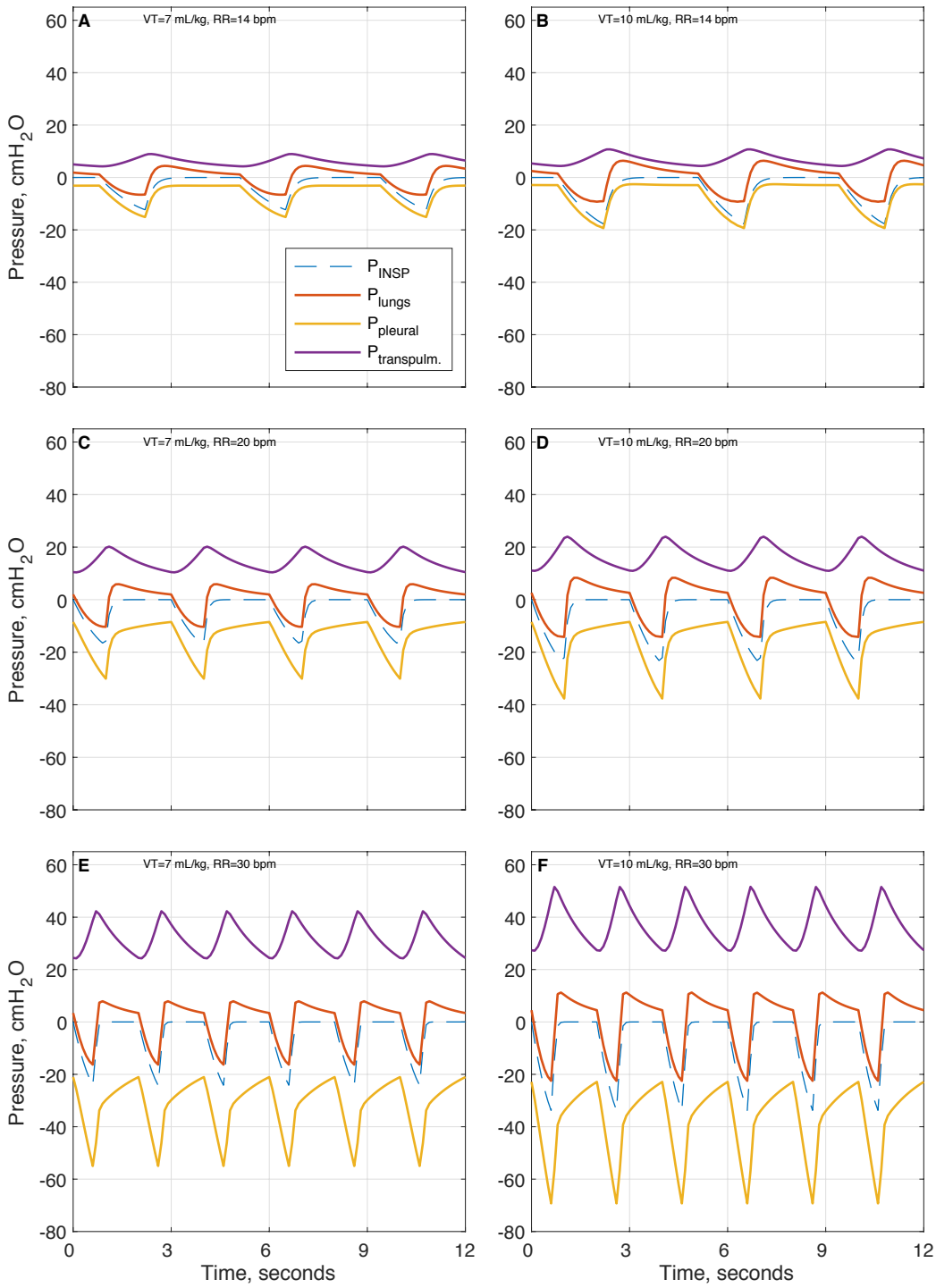

Figure 1: Inspiratory, pleural, transpulmonary and alveolar pressure swings generated by normal and increased respiratory effort in our COVID-19 model (patient 1 – see SM Table S5.1), (A) VT = 7 ml/kg, RR = 14 b/min, (B) VT = 10 ml/kg, RR = 14 b/min, (C) VT = 7 ml/kg, RR = 20 b/min, (D) VT = 10 ml/kg, RR = 20 b/min, (E) VT = 7 ml/kg, RR = 30 b/min, (F) VT = 10 ml/kg, RR = 30 b/min.